separations

MDPI

Article

Study on the Effects of Wet Flue Gas Desulfurization on Particulate Matter Emission from Industrial Coal-Fired Power Plants

Anyu Wang [1], Shuran Li [2,3,*], Qinzhen Zheng [1], Shuo Zhang [1], Shihao Zhang [1], Zhihao Wang [1], Zhen Liu [1] and Keping Yan [1,4,*]

[1] College of Chemical and Biological Engineering, Zhejiang University, Hangzhou 310028, China; anyu_wang@zju.edu.cn (A.W.)
[2] State Key Laboratory of Fluid Power and Mechatronic Systems, School of Mechanical Engineering, Zhejiang University, Hangzhou 310027, China
[3] Key Laboratory of Advanced Manufacturing Technology of Zhejiang Province, School of Mechanical Engineering, Zhejiang University, Hangzhou 310027, China
[4] Shanxi-Zheda Institute of Advanced Materials and Chemical Engineering, Taiyuan 030002, China
* Correspondence: lisr@zju.edu.cn (S.L.); kyan@zju.edu.cn (K.Y.)

Abstract: This study aimed to investigate the effects of wet flue gas desulfurization (WFGD) on particulate matter (PM) emissions in coal-fired power plants (CFPPs) using an electrical low-pressure impactor (ELPI). The investigation was conducted on five industrial CFPPs of various loads in China to clarify the influence factors of WFGD on PM_{10} emissions. After WFGD, the proportion of $PM_{2.5}$ to PM_{10} in the outlet flue gas increases, which showed that the WFGD system is selective in the capture of PM, with a significant effect on the capture of large particle sizes. The investigation found that four spray layers have a better effect on the capture of particles than two spray layers. Additionally, the investigation also found that unit load is not the main factor affecting the efficiency of PM_{10} capture by WFGD. Instead, the factors affecting the capture efficiency of PM_{10} by WFGD are the inlet flue gas temperature and the dust concentration. Relatively higher inlet flue gas temperature and lower inlet dust concentration will both result in higher emission of $PM_{0.1\sim1}$ from the WFGD outlet. These findings suggest that a matched integration of WFGD and CFPP is essential for ultra-low PM emission control and green industry development.

Keywords: wet flue gas desulfurization (WFGD); particulate matter (PM); coal-fired power plant (CFPP); electrical low-pressure impactor (ELPI)

Citation: Wang, A.; Li, S.; Zheng, Q.; Zhang, S.; Zhang, S.; Wang, Z.; Liu, Z.; Yan, K. Study on the Effects of Wet Flue Gas Desulfurization on Particulate Matter Emission from Industrial Coal-Fired Power Plants. *Separations* **2023**, *10*, 356. https://doi.org/10.3390/separations10060356

Academic Editor: Dimosthenis Giokas

Received: 16 May 2023
Revised: 9 June 2023
Accepted: 11 June 2023
Published: 14 June 2023

1. Introduction

China has abundant coal reserves, and the country is one of the largest consumers of coal resources in the world. Coal-fired power plants (CFPPs) are one of the main sources of pollutants, including gaseous pollutant NO_x, SO_2, and particulate matter (PM), which are harmful for both the environment quality and human health [1,2]. PM, in particular, can accumulate toxic substances through respiratory exposure due to its high specific surface area and formation mechanism [3–6]. Given the significant impact of CFPPs on air quality, it is crucial to control their emissions of pollutants, especially PM smaller than 2.5 μm, from which we can reap significant economic and environmental benefits [7,8].

Hence, the Chinese government has been making CFPPs a key regulatory source for controlling air pollution [9]. In 2014, China issued the "Reformation and Upgrading Action Plan for Coal Energy Conservation and Emission Reduction (2014–2020)" [10], which requires ultra-low emission standards of less than 10, 35, and 50 mg/Nm^3 (standard temperature and pressure (273.15 K, 1 atm) with 6% O_2) for PM, SO_2, and NO_x, respectively. More stringently, dust emissions were required to be less than 5 mg/Nm^3.

In China, the control of three primary air pollutants—NO_x, PM, and SO_2—is a priority for coal-fired boilers. To achieve this, selective catalytic reduction (SCR), electrostatic precipitator (ESP), and wet flue gas desulfurization (WFGD) technologies are widely installed in sequence [11–14]. Although ESP can remove up to 99% of fly ash, it is less effective for fine particles (smaller than 2.5 μm), and achieving the 5 mg/Nm^3 emission standard is challenging [15–17]. Since the first successful ultra-low emission CFPPs demonstration in 2014 [18], research on PM emissions has been increasing. Studies of CFPP emissions suggest that the comparison of fine and coarse particle ratios may vary depending on the treatment or source of the emissions [19], but the dominance of fine particles is dangerous to human health [20] because fine particles can penetrate more deeply into the lungs than coarse particles [21].

In general, there is a strong association between sulfur dioxide emissions and particulate matter: fuels containing high levels of sulfur are associated with high levels of sulfate and ash, which increase the organic particulates produced during combustion, and higher sulfur levels in fuels are also associated with larger particle sizes [22]. There are dry desulfurization, semi-dry desulfurization, and wet desulfurization technologies for flue gas desulfurization. In China, WFGD technology is a more mature and widely used desulfurization technology, which uses a liquid desulfurizer, so it uses alkaline liquid desulfurizer to absorb SO_2 in the flue gas [23], such as limestone-gypsum desulfurization [24], double alkali desulfurization [25], magnesium oxide desulfurization [26], etc. Wet electrostatic scrubbing (WES) and WFGD technology can remove dust to some extent while desulfurizing [27]. Previous studies have investigated the removal efficiency of WFGD for PM in different units. For instance, Liu et al. [28] reported WFGD removal efficiencies of 28.7% and 39.6% for $PM_{0.1}$ and $PM_{2.5}$, respectively, in a 1000 MW unit. Li et al. [29] investigated the concentration and composition of PM in ultra-low emission power plants and the overall PM elimination efficiency was extremely good for the combination of ESP, WFGD, and WESP. Sui et al. [30] investigated the distribution and composition of PM_{10} imported and exported from ESP, WFGD, and WESP after the ultra-low emission retrofit and it was found that the combined application of low-temperature economizer, retrofitted ESP, FGD, and WESP can reduce fine particle emissions from coal-fired power plants to less than 1 mg/m^3. Wu et al. [31] proposed a non-homogeneous condensation process of limestone-gypsum desulfurization combined with waste heat recovery, and the results showed that the inlet flue gas with high relative humidity can remove fine particulate matter, and the high liquid-gas ratio of WFGD system is also beneficial to the effective removal of fine particulate matter. Yang et al. [32] investigated the control of pollutants in coal-fired power plants by WFGD and WESP. The removal efficiencies of PM_{10} by WFGD and WESP were 64.0–70.3% and 57.5–79.2%, respectively, with WFGD having a greater effect on the particle size distribution. The studies mainly focused on one or two plants, and little attention was paid to the factors influencing WFGD efficiency for dust removal.

The main goal of this research was to investigate the effects of WFGD systems on PM emission, including PM_{10} and $PM_{2.5}$ concentration, diameter distribution, and their ratio, in WFGD systems in five industrial CFPPs of different loads in China, using an electrical low-pressure impactor (ELPI) system to measure particle size distribution at the inlet and outlet of the WFGD. The five CFPPs were selected to represent coal-fired boilers for ultra-low emission retrofit in China, ranging from a 75 t/h industrial boiler to 600 MW units. The study analyzed the grade efficiency and emission ratio of particles with different diameters. Additionally, the effect of spray layer amount, inlet flue gas temperature, and dust concentration on PM_{10} emissions from the wet desulfurization outlet was investigated in four 330 MW units at Power Plant C. This study provides practical data covering plants of multiple types and investigates various factors affecting the efficiency of WFGD for dust removal. This study provided a large amount of data based on actual industrial boiler applications, and the effect factors of the combination of ESP and FGD have been evaluated; more importantly, the contribution of different operating parameter has been tested, which can be used to improve the design and operation of the integration of WFGD and ESP

systems in CFPPs, ultimately reducing the emission of harmful pollutants and protecting the environment and human health.

2. Experimental Section

2.1. APCDs in the CFPPs

This study conducted tests on the PM_{10} mass concentrations at the inlet and outlet of wet desulfurization towers in five coal-fired power plants in China, with unit loads ranging from 75 t/h to 600 MW. These plants represent the ultra-low emission retrofit of coal-fired boilers in China. This study included detailed information on the characteristics of each plant, as shown in Table 1, including the air pollution control devices (APCDs) installed in each, such as SCR for NO_x control, low-temperature economizer (LTE) for heat utilization, ESP for particle removal, and WFGD for the further reduction of PM and SO_3 emissions. Figure 1a provides a schematic diagram of the APCDs and sampling points in the CFPPs. The ELPI system was used to sample particles and measure the particle size distribution. This study also investigated the effect of different inlet flue gas temperatures and concentrations and the number of spray layers on PM_{10} emissions from the wet desulfurization outlet in four 330 MW units at Power Plant C. Overall, the study aimed to analyze the emission and removal characteristics of PM_{10} in WFGD and provide information on factors affecting the efficiency of WFGD for dust removal.

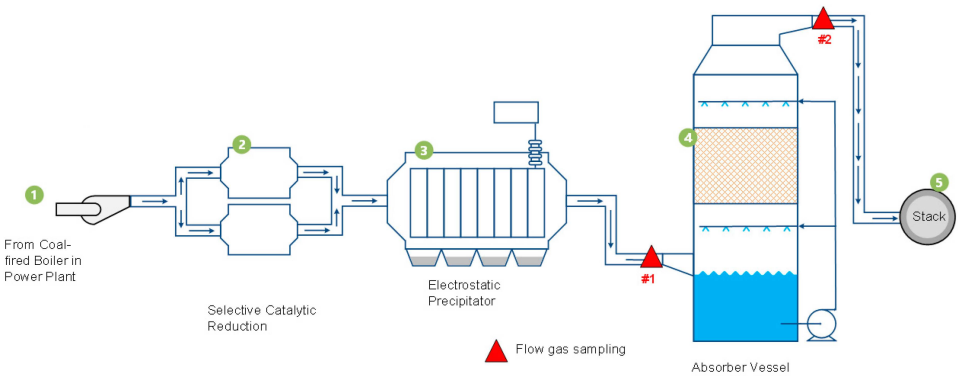

(a)

(b)

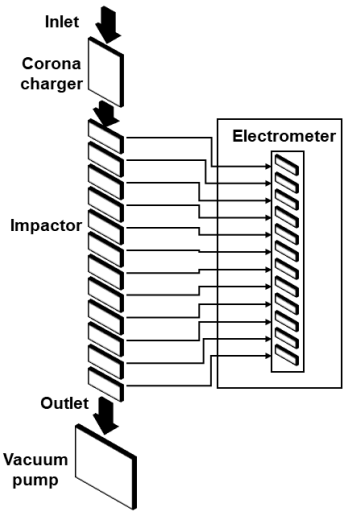

(c)

Figure 1. (**a**) Schematic configuration of APCDs and sampling points of the tested CFPPs; (**b**) electrical low-pressure impactor (ELPI) for particles concentration test; and (**c**) schematic configuration of ELPI.

Table 1. Description of the studied plants.

Description	Plant A	Plant B	Plant C	Plant D	Plant E
boiler type	CFB boiler	PC boiler	PC boiler	PC boiler	CFB boiler
installed capacity (MW)/BMCR (t/h)	3 × 15/75	4 × 220/670	4 × 330/1100	2 × 600/1900	2 × 135/440
flue gas flow ($\times 10^4$ m^3/h)	10	45	110	145	88
flue gas temperature (°C)	140	95	140 (110)	-	120
mist eliminator type	Tubular type	2nd roof ridge type	3rd roof ridge type	3rd roof ridge type	3rd roof ridge type+ Mechanical grille type
APCDs	SCR + ESP + WFGD	SCR + LTE + ESP + WFGD	SCR + (LTE) + ESP + WFGD	SCR + ESP + WFGD	SCR + LTE + ESP + WFGD

2.2. Total Particle Concentration and Flue Gas Temperature Test

The test method for total PM concentration in this paper mainly refers to China's "Sampling Method for Particulate Matter and Gaseous Pollutants in Exhaust from Stationary Sources" GB/T16157-1996 [33], using the Pitot tube dynamic pressure balance isometric sampling method. The instrument used in this study for the testing of total particulate matter concentration was a Pitot tube parallel automatic smoke sampler, model WJ-60B, produced by Qingdao Laoshan Electronic Instrument General Factory Co. (Qingdao, China), and the main technical specifications of the sampler are shown in Table 2. The sampler is also equipped with a temperature sensor for testing the flue gas temperature while testing the PM concentration.

Table 2. Main technical specifications of WJ-60B sampler.

Description	Range	Resolution	Accuracy
Sampling flow rate	5~60 L/min	0.1 L/min	±2.5%
Isometric sampling flow rate	1~45 m/s	0.1 m/s	<±4%
Flue gas dynamic pressure	0 Pa~2000 Pa	1 Pa	<±1.5%
Flue gas static pressure	−20 kPa~20 kPa	0.01 kPa	<±4%
Flue gas full pressure	−20 kPa~20 kPa	0.01 kPa	<±4%
Pressure before flow meter	−30 kPa~0 kPa	0.01 kPa	<±2.5%
Temperature before flow meter	−20 °C~100 °C	0.1 °C	<±1.5%
Flue gas temperature	0 °C~500 °C	1 °C	≤±3 °C
Dry bulb temperature	0~100 °C	0.1 °C	
Wet bulb temperature	0~100 °C	0.1 °C	
Humidity content	0~60%	0.1%	<±1.5%

2.3. PM_{10} Graded Concentration Test

In this study, the particle size distribution of PM_{10} was measured using an ELPI from DEKATI, Finland, which combines electrical detection with a conventional cascade impactor to acquire real-time aerosol measurement [34]. The ELPI is capable of the real-time measurement of both number and mass particle size distribution [35]; the main specifications of ELPI are shown in Table 3. Figure 1b,c show the schematic diagram of the ELPI, which consists of a charger and a sampler. The particles are charged in the charger and then enter the sampler, which has 12 independent sampling trays with microcurrent probes. The microcurrent probes capture the current signal and convert it into particle size distribution.

In addition, the ELPI was compared to the results of simultaneous sampling tests with conventional membrane and cartridge sampling guns under the same flue gas conditions in order to show the stability and reliability of ELPI. In Plant E, a filter membrane sampler and a filter cartridge sampler were used alongside ELPI. Each test was conducted simultaneously under the same flue gas conditions for a duration of 50 min. The conventional samplers pumped approximately 1000 L of gas while the ELPI recorded 3000 data points at a rate of one test result per second. The distribution of the flue gas flow field at the sampling point is not entirely uniform, causing fluctuations in the dust concentration.

Therefore, the average of continuous 60 data points was used to determine the average mass concentration of PM per minute.

Table 3. Main technical specifications of ELPI.

Description	Range
Rated flow rate	10 L/min
Range of particle size	0.03~10 μm
Number of sampling trays	12
Operating temperature	5~40 °C
Operating humidity	0~60% RH
Flue gas temperature	−30 kPa–0 kPa
First stage sampling tray pressure	100 mBar
Response time	<5 s

2.4. Particle Matter Sampling Description

The particle size distributions (PSDs) are presented with the expression of D_p—dM/dlog(D_p) [36]:

$$dM/d\log(D_p) = \frac{\Delta M}{\log D_{p,upper} - \log D_{p,lower}} \quad (1)$$

where D_p is the aerodynamic diameter, μm. ΔM (mg·m^{-3}) is the mass concentration in each stage. log $D_{p,upper}$ and log $D_{p,lower}$ are the upper and lower cut-off diameters of each stage, respectively.

Based on the mass concentration of PM, the grade efficiency η can be obtained using the following expression [37]:

$$\eta = \frac{c_{inlet} - c_{outlet}}{c_{inlet}} \times 100\% \quad (2)$$

where c_{inlet} and c_{outlet} are the mass concentrations of PM at the inlet and outlet of WFGD in mg/m^3, respectively.

3. Results and Discussion

3.1. Comparison of ELPI and Conventional Sampler

The results of the comparison indicated that the PM_{10} mass concentration ranged from 1 mg/m^3 to 7 mg/m^3, with an average value of 2.84 mg/m^3 and a mean square deviation of 77%, demonstrating the reliability of the ELPI measurement.

The real-time and every minute test results of ELPI are shown in Figure 2a. The PM concentration varied smoothly between 2 mg/m^3 to 4 mg/m^3. The ELPI instrument can be considered a reliable method of expressing dust concentration, as the average concentration in any 60-s period only varies by 2 mg/m^3.

To compare the data obtained from ELPI with traditional sampling methods, the study divided the 3000-s ELPI data into six parts and calculated their average values separately. As shown in Figure 2b, three out of five tests using the filter cartridge sampler resulted in negative concentrations, with a mean value of −0.44 mg/m^3 and a mean square deviation of 151%. Two out of five tests using the filter membrane sampler also resulted in negative concentrations, with a mean value of 2.02 mg/m^3 and a mean square deviation of 518%. In contrast, all six groups of data sampled using ELPI were positive, with a mean value of 2.84 mg/m^3 and a mean square deviation of 56.7%. Therefore, the test results of the traditional filter membrane sampler and filter cartridge sampler were highly deviated and lacked credibility. On the other hand, the test results obtained from ELPI were evenly distributed, showed a smooth change trend, and had little deviation. As a result, ELPI was used for all soot concentration tests in this study.

Using ELPI, Figure 2c,d display the mass concentration and ratio of $PM_{2.5}$ and PM_{10} at the inlet of the WFGD at different operating capacities, as well as the mass concentration of $PM_{2.5}$ and PM_{10} at the inlet of the WFGD in different plants.

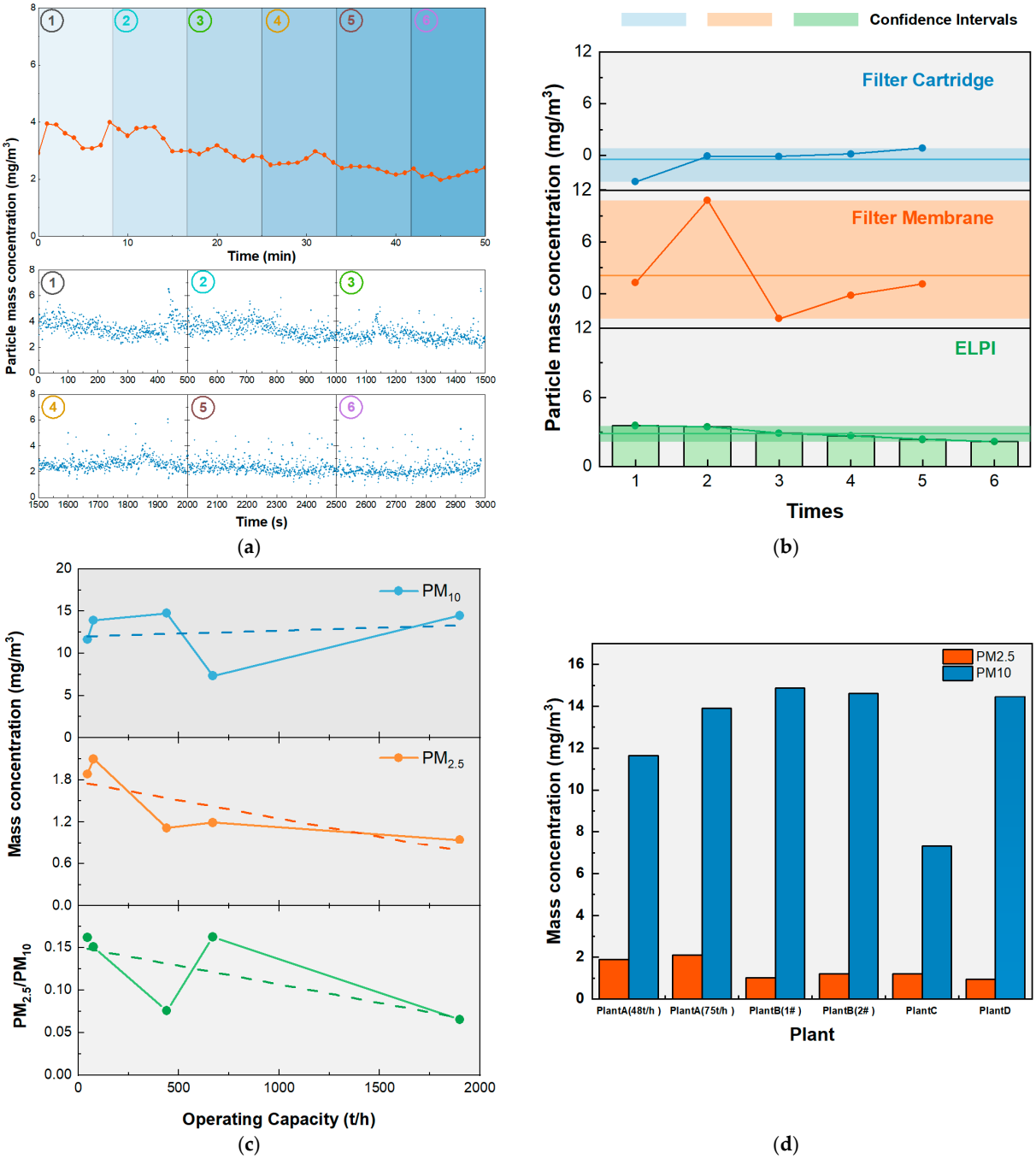

Figure 2. (**a**) Real-time and every minute test results of ELPI; (**b**) sampling results with different samplers; (**c**) mass concentration and ratio of $PM_{2.5}$ and PM_{10} at the inlet of the WFGD with different operating capacity; and (**d**) mass concentration of $PM_{2.5}$ and PM_{10} at the inlet of the WFGD in different plants, 1# and 2# denote the two identical units of Plant B.

3.2. Characteristics of PM Emission at the Inlet and Outlet of the Industrial Boiler

Plant A has an industrial boiler with a rated evaporation capacity of 75 t/h. To examine the changes in PM concentration after wet desulfurization under different concentration conditions at the desulfurization inlet, two boiler loads (high and low) of 75 t/h and 48 t/h,

respectively, were used during the experiment. Figure 3a,b illustrate the particle size distribution and grade efficiency in the desulfurization process for Plant A at 48 t/h and 75 t/h loads.

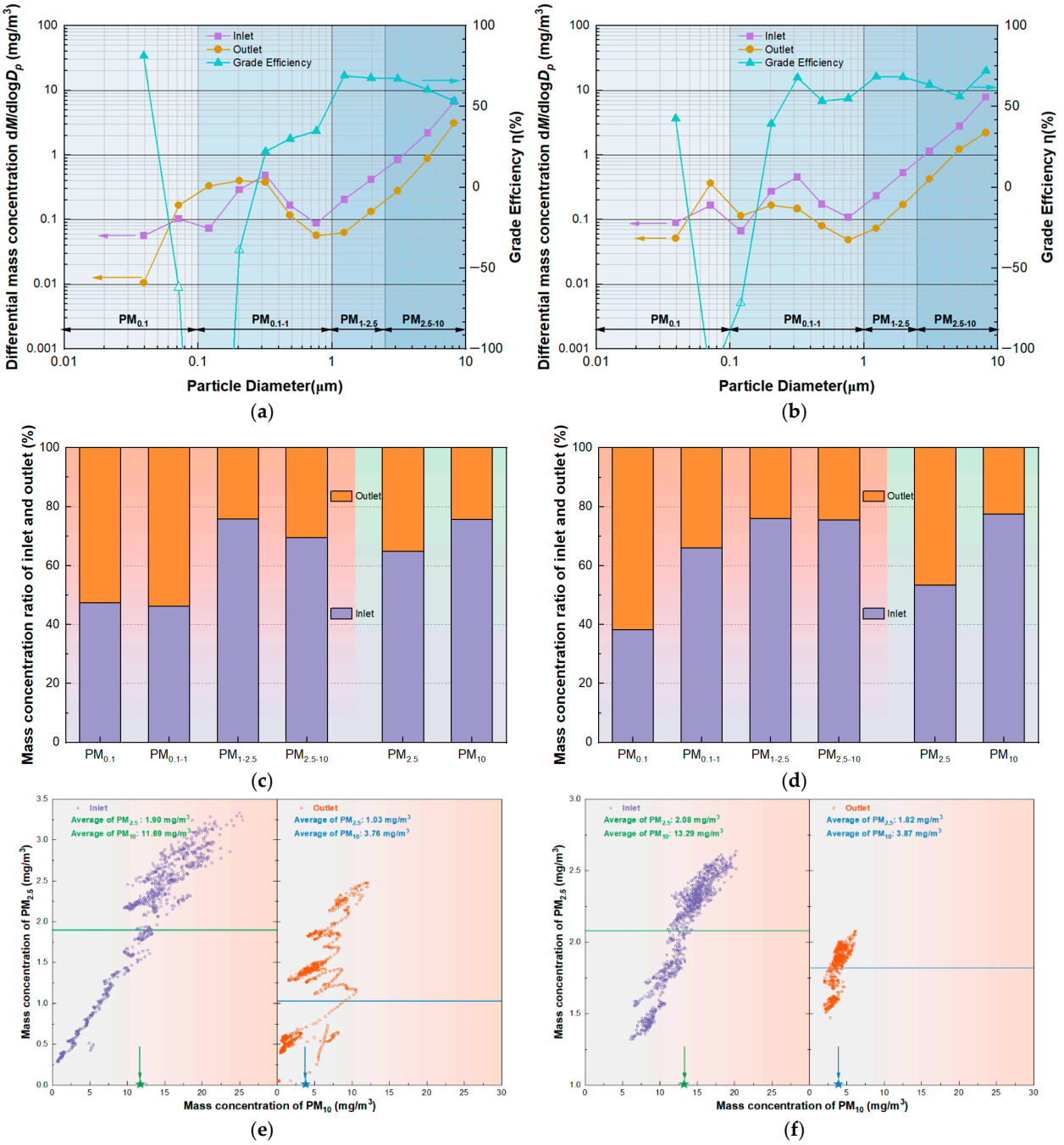

Figure 3. Particle size distributions and grade efficiency of PM_{10} in the desulfurization process for Plant A at (**a**) 48 t/h and (**b**) 75 t/h load; emission ratio of particles with different diameter at inlet and outlet of WFGD for Plant 1 at (**c**) 48 t/h and (**d**) 75 t/h load; real-time distribution of mass concentration of PM_{10} and $PM_{2.5}$ at the inlet and outlet of WFGD for Plant A at (**e**) 48 t/h and (**f**) 75 t/h load.

3.2.1. For Plant A at 48 t/h Load

At 48 t/h load, the WFGD tower had a PM_{10} mass concentration of 11.69 mg/m^3 at the inlet and 3.76 mg/m^3 at the outlet, with a capture efficiency of 67.84% for PM_{10}. The

$PM_{2.5}$ mass concentration at the inlet was 1.90 mg/m^3, which reduced to 1.03 mg/m^3 at the outlet. The capture efficiency of the WFGD tower for $PM_{2.5}$ was 45.79%.

Figure 3c illustrates the emission ratio of particles with different diameters at the inlet and outlet of WFGD for Plant A, at 48 t/h load. The mass concentration of $PM_{1\sim10}$ decreased the most, by approximately 39.7%, followed by $PM_{0.5\sim1}$, which decreased by about 21.1% after desulfurization. However, both $PM_{0.1}$ and $PM_{0.1\sim0.5}$ showed a slight increasing trend after the process.

Figure 3e depicts the real-time distribution of mass concentration of PM_{10} and $PM_{2.5}$ at the inlet and outlet of WFGD for Plant A. At the lower load, the average mass concentrations of $PM_{2.5}$ were 1.90 mg/m^3 and 1.03 mg/m^3 at the inlet and outlet, respectively, whereas the average mass concentrations of PM_{10} were 11.69 mg/m^3 and 3.76 mg/m^3 at the inlet and outlet, respectively. The mass concentration ratio of $PM_{2.5}$ to PM_{10} was 16.25% at the inlet and 27.39% at the outlet.

3.2.2. For Plant A at 75 t/h Load

At 75 t/h load, the PM_{10} mass concentration of the WFGD tower at the inlet and outlet were 13.29 mg/m^3 and 3.87 mg/m^3, respectively. The WFGD tower had a capture efficiency of 70.88% for PM_{10}. The $PM_{2.5}$ mass concentration at the inlet was 2.08 mg/m^3, which reduced to 1.82 mg/m^3 at the outlet. However, the capture efficiency of the WFGD tower for $PM_{2.5}$ was only 12.50%.

Figure 3d illustrates the emission ratio of particles with different diameters at the inlet and outlet of WFGD for Plant A, at 75 t/h load. All $PM_{0.1\sim10}$ mass concentrations decreased, with $PM_{0.1}$ mass concentration increasing after desulfurization. After the desulfurization process, the mass concentration of $PM_{1\sim10}$ changed significantly, whereas the change in PM_1 mass concentration was relatively small. However, $PM_{0.5}$ mass concentration showed an increasing trend, primarily due to the uneven distribution of local airflow in the desulfurization tower, resulting in an increased secondary carryover of desulfurization slurry, and leading to increased particle emissions in $PM_{0.5}$.

Figure 3f depicts the real-time distribution of mass concentration of PM_{10} and $PM_{2.5}$ at the inlet and outlet of WFGD for Plant A. At the higher load, the average mass concentrations of $PM_{2.5}$ were 2.08 mg/m^3 and 1.82 mg/m^3 at the inlet and outlet, respectively, whereas the average mass concentrations of PM_{10} were 13.29 mg/m^3 and 3.87 mg/m^3 at the inlet and outlet, respectively. The mass concentration ratio of $PM_{2.5}$ to PM_{10} was 15.65% at the inlet and 47.03% at the outlet. The ratio increased in the outlet due to the higher capture efficiency of $PM_{1\sim10}$ by WFGD and the large proportion of $PM_{1\sim10}$ in PM_{10}.

The WFGD process effectively captures PM_{10}, resulting in a more concentrated real-time distribution of $PM_{2.5}$ and PM_{10} mass concentrations. Notably, the capture efficiency of PM_{10} is closely related to the boiler load. As the load increases, the mass concentration of PM_{10} at the inlet also increases, but so does the capture efficiency. The higher the operating load, the higher the particulate capture efficiency for the same APCD case, which is consistent with the results of previous studies [29]. However, changes in boiler load do not appear to affect the particle size distribution characteristics of PM_{10} before and after desulfurization.

3.3. Characteristics of PM Emission at the Inlet and Outlet of Coal-Fired Boilers

3.3.1. For Plant B with 220 MW

Plant B has a rated generating capacity of 220 MW and was operated at full load during the experiment. Figure 4a illustrates the particle size distribution and grade efficiency of PM_{10} at the inlet and outlet of WFGD. The results show that the mass concentration of $PM_{0.1\sim5}$ increased to varying degrees. The PM_{10} mass concentration at the WFGD tower was 7.78 mg/m^3 at the inlet and 7.45 mg/m^3 at the outlet, with a capture efficiency of 4.24% for PM_{10}. The $PM_{2.5}$ mass concentration was 1.29 mg/m^3 at the inlet and 1.36 mg/m^3 at the outlet, representing a 5.14% increase. Figure 4b presents the emission ratio of particles with different diameters at the inlet and outlet of WFGD for Plant B. The results show

that after desulfurization, the mass concentration of $PM_{0.1}$ significantly reduced by 93.7%, with an absolute value of 0.0364 mg/m^3. However, the mass concentrations of $PM_{0.1\sim10}$ all increased to varying degrees, with the mass concentration of $PM_{0.1\sim1}$ increasing by 149.21%, $PM_{1\sim2.5}$ increasing by 29.63%, and $PM_{2.5\sim10}$ increasing by 5.08%.

The real-time distribution of mass concentration of $PM_{2.5}$ and PM_{10} at the inlet and outlet of the WFGD were analyzed, as shown in Figure 4c, indicating that the distribution range of PM_{10} mass concentration before and after desulfurization is very similar. The average mass concentrations of $PM_{2.5}$ were 1.29 mg/m^3 at the inlet and 1.36 mg/m^3 at the outlet, whereas the average mass concentrations of PM_{10} were 7.78 mg/m^3 at the inlet and 7.45 mg/m^3 at the outlet. The mass concentration ratio of $PM_{2.5}$ to PM_{10} was 16.58% at the inlet and 18.26% at the outlet. These results indicate that $PM_{2.5}$ constitutes a larger proportion of PM_{10} after wet desulfurization, which is consistent with the conclusion of previous studies that ESP and WFGD are more effective in removing coarse particles than fine particles [32,37,38].

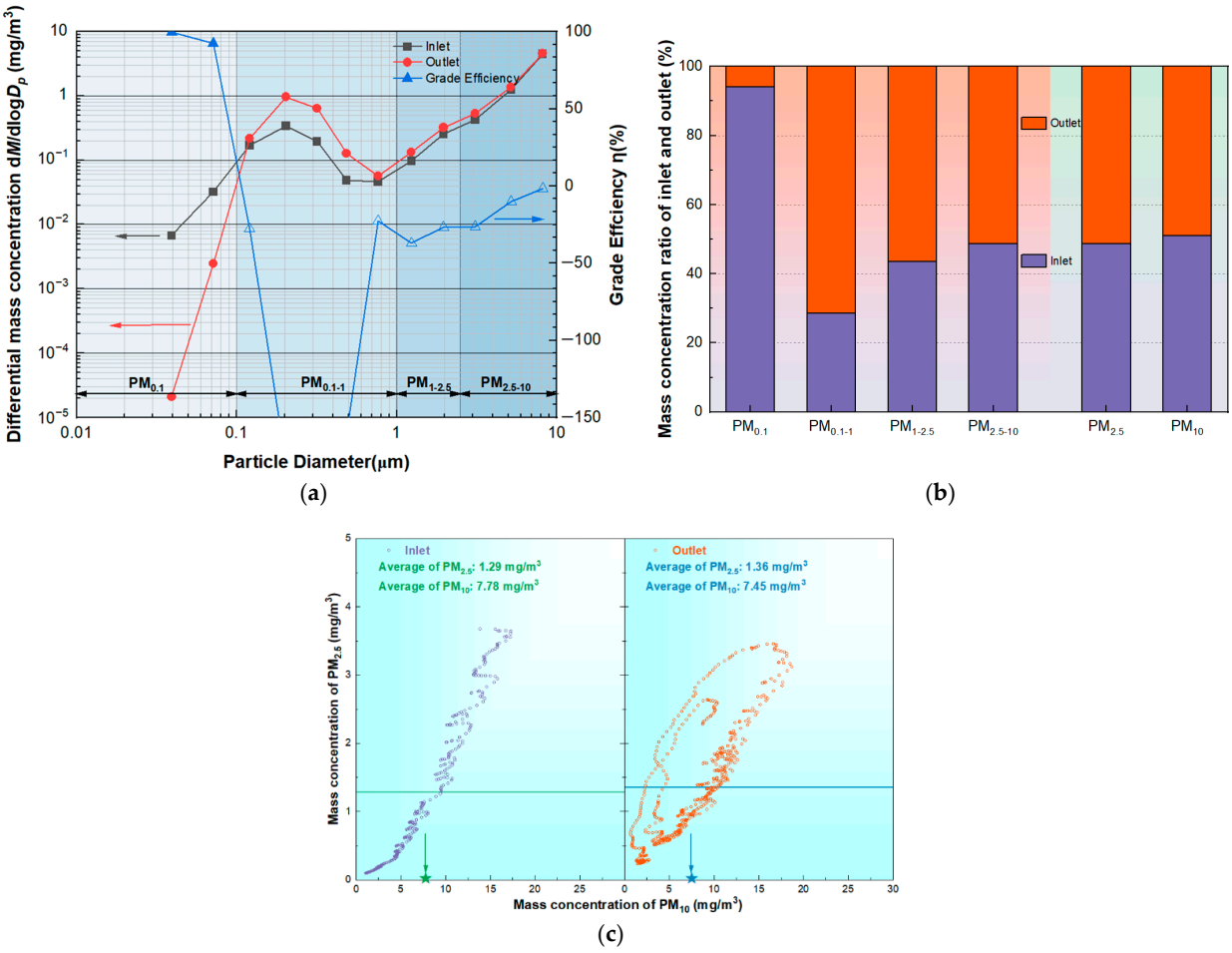

Figure 4. (**a**) Particle size distributions and grade efficiency of PM_{10}, (**b**) emission ratio of particles with different diameter, and (**c**) real-time distribution of mass concentration of PM_{10} and $PM_{2.5}$ at the inlet and outlet of WFGD for Plant B.

3.3.2. For Plant E with 135 MW

Plant E comprises two 135 MW coal-fired units that are structurally identical with the same size of WFGD towers and similar flue gas operating conditions, with the only difference being the mist eliminator. Specifically, Unit 1 uses a three-stage roof mist eliminator, whereas Unit 2 still employs the traditional mechanical grille mist eliminator. This study focuses on comparing the performance of the two mist eliminators under the same operating conditions.

According to Figure 5a,c, the PM_{10} mass concentration distribution at the WFGD inlet is similar for both Unit 1 and Unit 2 under the same operating conditions, with PM_{10} mass concentrations of 14.87 mg/m^3 and 15.26 mg/m^3, respectively. The $PM_{2.5}$ mass concentrations for Unit 1 and Unit 2 are 1.02 mg/m^3 and 1.23 mg/m^3, respectively, and the $PM_{2.5}$ mass concentrations as a percentage of PM_{10} are 6.86% and 8.06%, respectively. Figure 5b shows that after wet desulfurization, the $PM_{2.5}$ outlet mass concentration increased in both Unit 1 and Unit 2 by 9.80% and 69.10%, respectively. The PM_{10} outlet mass concentration of Unit 1 decreased by 51.71%, whereas that of Unit 2 increased by 53.93%.

Additionally, Figure 5c shows the real-time mass concentration distribution of $PM_{2.5}$ and PM_{10} at the WFGD inlet and outlet of Unit 1 and Unit 2. The PM_{10} mass concentration at the WFGD tower outlet of Unit 2 with the traditional mechanical grille mist eliminator is highly dispersed, with the instantaneous mass concentration of PM_{10} reaching up to 150 mg/m^3, the instantaneous mass concentration of $PM_{2.5}$ up to 10 mg/m^3, and the average mass concentration of $PM_{2.5}$ accounting for 8.85% of PM_{10}. In contrast, the PM_{10} mass concentration at the outlet of the WFGD tower of Unit 1 with the three-stage roof-type mist eliminator is more concentrated, and the average mass concentration of $PM_{2.5}$ is 15.60% of PM_{10}.

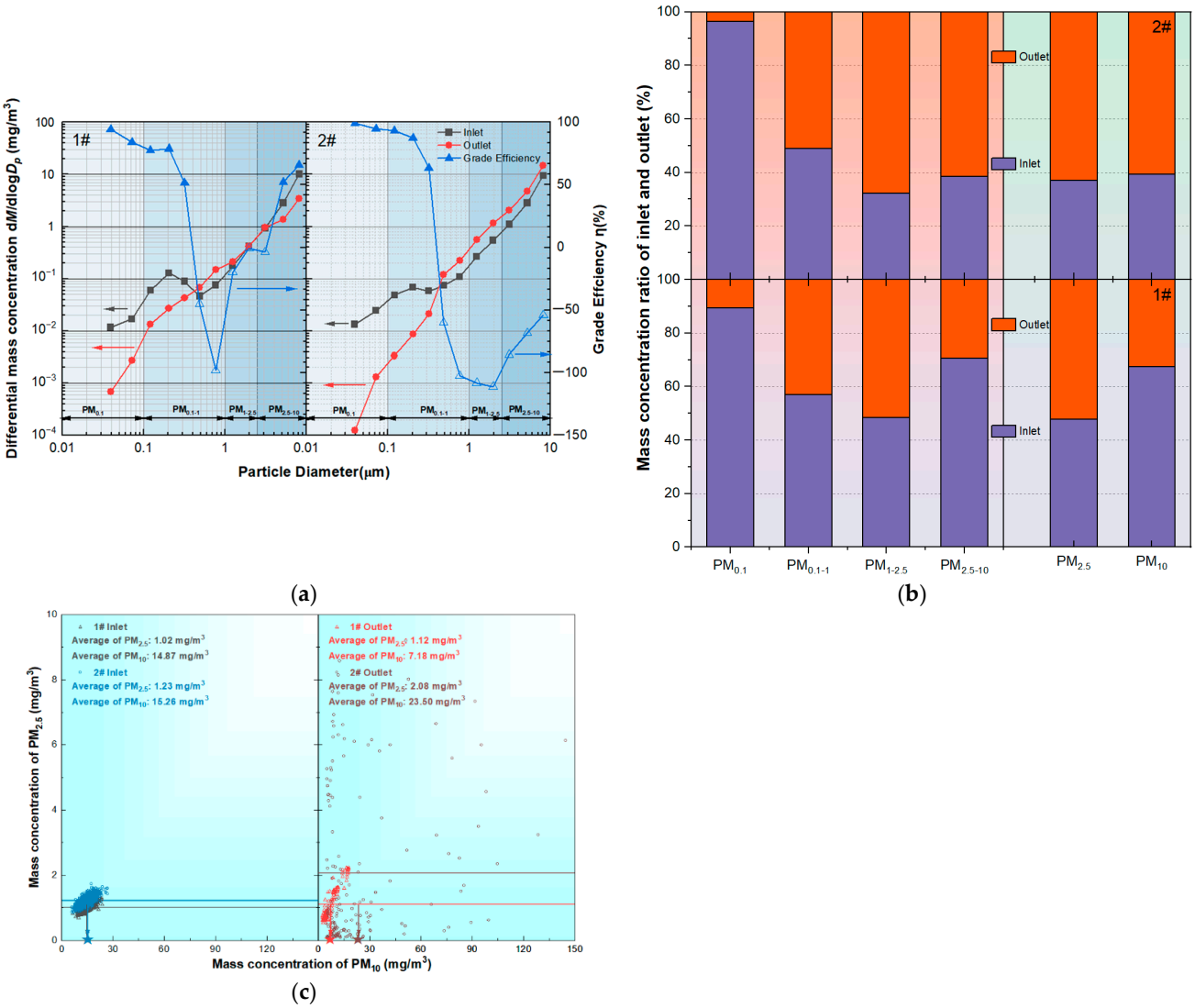

Figure 5. (**a**) Particle size distributions and grade efficiency of PM_{10}, (**b**) emission ratio of particles with different diameter, and (**c**) real-time distribution of mass concentration of PM_{10} and $PM_{2.5}$ at the inlet and outlet of WFGD for Unit 1 and Unit 2 of Plant E.

Moreover, the movement of different particle sizes is influenced by different flow fields. The flow field inside the traditional mechanical grille mist eliminator is relatively smooth and uniform. $PM_{0.5\sim10}$ particles are subject to significant flow field traction, making it easier for them to escape from the mist eliminator by following the flow field. $PM_{0.5}$ particles are subject to less flow field traction, but due to their Brownian motion and electrostatic effects, the probability of collision with the surface of the mechanical grille mist eliminator increases.

In conclusion, the traditional mechanical grille has a higher capture efficiency for $PM_{0.5}$ particles. On the other hand, the three-stage ridge type mist eliminator has a higher capture efficiency for $PM_{0.5\sim10}$ particles.

3.3.3. For Plant D with 600 MW

Plant D comprises two 600 MW coal-fired units. The real-time mass concentration curves of PM_{10} and $PM_{2.5}$ at the inlet and outlet of WFGD, using an ELPI instrument, are presented in Figure 6a. The smoothness of the curves indicates the accuracy and stability of the ELPI-based thermostatic and dilution sampling method for testing PM_{10} of high temperature and high humidity flue gas. Figure 6b presents the particle size distributions and grade efficiency of PM_{10}. At the WFGD inlet, the PM_{10} mass concentration was 14.48 mg/m^3, with a $PM_{2.5}$ mass concentration of 0.94 mg/m^3, accounting for 6.49% of PM_{10}. At the WFGD outlet, the PM_{10} mass concentration was 3.09 mg/m^3, with a $PM_{2.5}$ mass concentration of 0.62 mg/m^3, accounting for 20.06% of PM_{10}, which was 13.57% higher than that at the WFGD inlet. The capture efficiency of WFGD for PM_{10} was 78.66% and for $PM_{2.5}$ was 34.04%. Figure 6c shows the emission ratio of particles with different diameters, highlighting that the capture efficiency for $PM_{0.1\sim1}$ is relatively low, whereas that for $PM_{0.1}$ and $PM_{1\sim10}$ is relatively high. Figure 6d presents the real-time distribution of the mass concentration of PM_{10} and $PM_{2.5}$ at the inlet and outlet of WFGD of Plant D, revealing a more concentrated and credible range of $PM_{2.5}$ and PM_{10} mass concentration distribution at the WFGD inlet and outlet.

3.4. Influencing Factors of PM_{10} Emissions from Wet Desulfurization

Plant C has four 330 MW coal-fired units, all of which have undergone ultra-low emission retrofit. This study examines the PM_{10} capture characteristics of wet desulfurization, focusing on the following factors: (1) number of spray layers, (2) flue gas temperature at the desulfurization inlet, and (3) PM concentrations at the desulfurization inlet. The emission concentrations of particulate matter for each unit were monitored after the completion of the retrofit.

3.4.1. The Influence of the Number of Spraying Layers

Experiments were conducted in the Unit 1 WFGD tower of Plant C to compare the capture efficiency of different numbers of spraying layers. The WFGD inlet mass concentration of PM_{10} was kept constant, and the distribution of PM_{10} mass concentration at the WFGD outlet was compared under two and four spraying layers by shutting down the corresponding slurry circulation pumps. Figure 7a shows the particle size distribution and grade efficiency at different numbers of spraying layers. The PM_{10} mass concentration was 14.36 mg/m^3 at the WFGD inlet, with $PM_{2.5}$ mass concentration accounting for 12.81% of PM_{10}, and the $PM_{2.5}$ mass concentration was 1.84 mg/m^3. Figure 7a,b indicate that the capture efficiency of WFGD is relatively poor for $PM_{1\sim2.5}$ and more efficient for $PM_{0.1}$ and $PM_{2.5\sim10}$. The overall PM_{10} grade efficiency improves when the number of spray layers is increased from two to four. Figure 7c shows the real-time distribution of mass concentration of PM_{10} and $PM_{2.5}$ at the inlet and outlet of the four spraying layers of Plant C. The PM_{10} mass concentration was 4.05 mg/m^3, with $PM_{2.5}$ mass concentration accounting for 29.38% of PM_{10}, and $PM_{2.5}$ mass concentration was 1.19 mg/m^3 at the outlet of WFGD of four spraying layers. The capture efficiency of PM_{10} in the four-layer spraying WFGD tower is 71.80%, and the capture efficiency of $PM_{2.5}$ is 35.33%. Additionally, the mass concentration

distribution of PM_{10} in the WFGD outlet is extremely concentrated, indicating that the capture efficiency of PM_{10} in the four-layer spraying is extremely high and stable. However, compared to two sprays, in the case of four sprays, the submicron PM concentration at the outlet is higher and the $PM_{0.1}$ capture efficiency decreases because more small droplets are entrained by the flue gas, leading to an increase in fine particulate matter [32]. Small droplets cannot be fully captured by the mist eliminator, and some of them penetrate, leading to an increase in submicron particles [39].

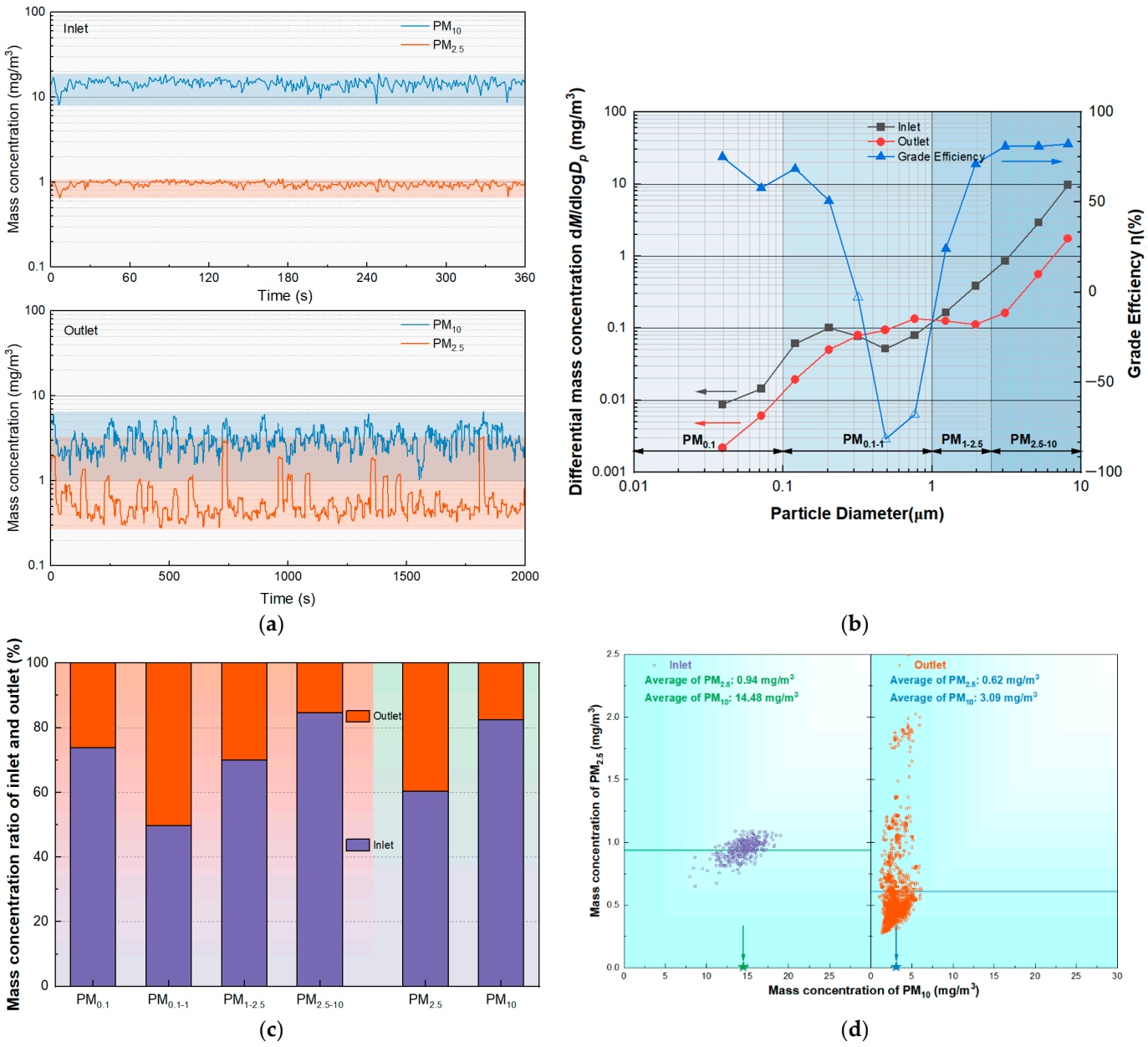

Figure 6. (**a**) Real-time test results at the inlet and outlet, (**b**) particle size distributions and grade efficiency of PM_{10}, (**c**) emission ratio of particles with different diameter, and (**d**) real-time distribution of mass concentration of PM_{10} and $PM_{2.5}$ at the inlet and outlet of WFGD of Plant D.

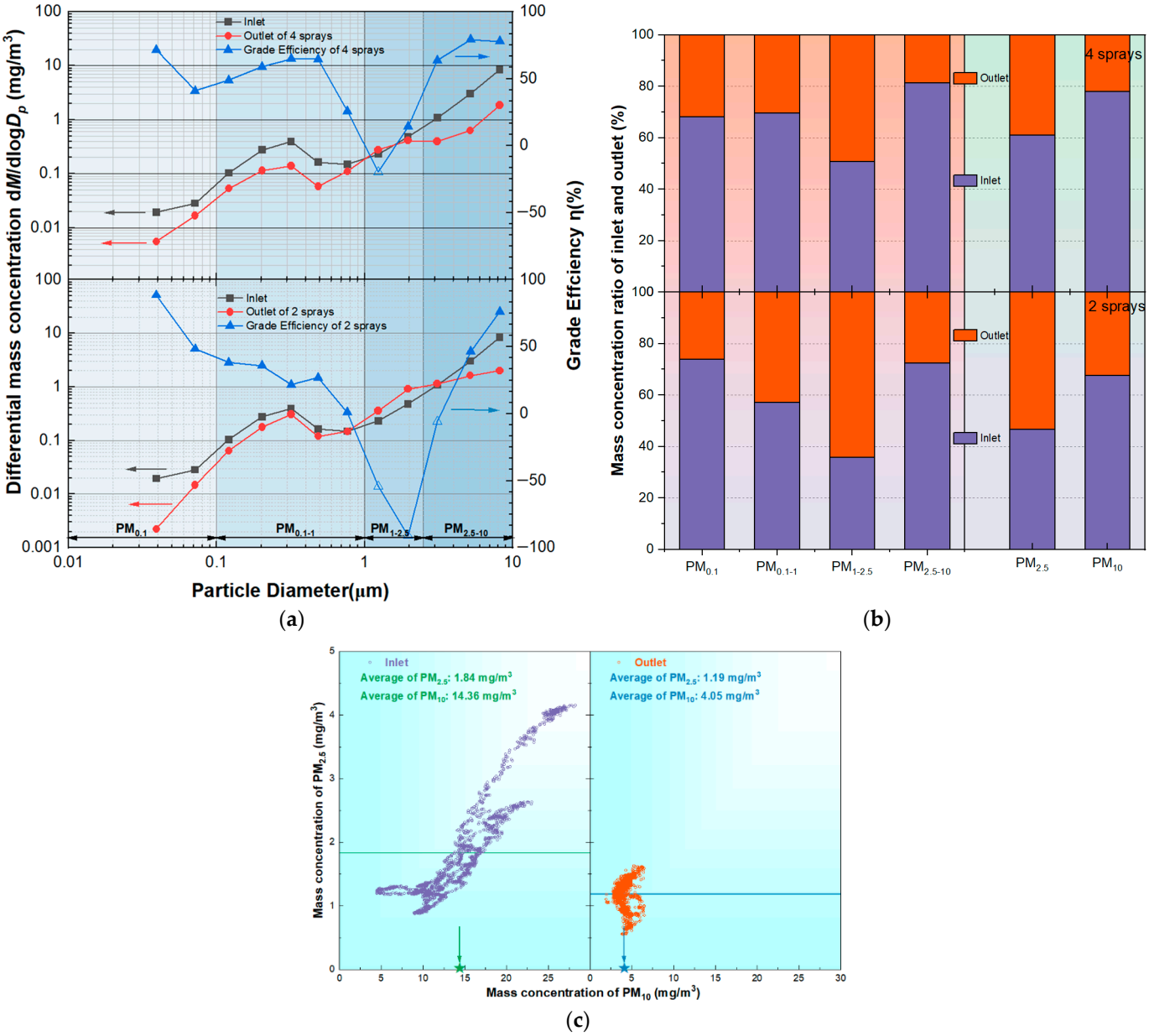

Figure 7. (**a**) Particle size distributions and grade efficiency of PM_{10} of two and four spraying layers, (**b**) emission ratio of particles with different diameter of two and four spraying layers, (**c**) real-time distribution of mass concentration of PM_{10} and $PM_{2.5}$ at the inlet and outlet of four spraying layers of Plant C.

3.4.2. The Influence of the Temperature of Inlet Flue Gas

The WFGD of Unit 2 in Power Plant C had an inlet flue gas temperature of 140 °C, and a low-temperature economizer was later added to the inlet of the electric precipitator. The inlet flue gas temperature dropped to 100 °C after the addition, and the flue gas temperature at the outlet of the desulfurization tower remained relatively stable. Figure 8a presents the particle size distributions and grade efficiency of PM_{10}. At the flue gas temperature of 140 °C, the total mass concentration of PM_{10} at the inlet of desulfurization was 17.37 mg/m^3, whereas the total mass concentration of $PM_{2.5}$ was 2.06 mg/m^3, and the ratio of $PM_{2.5}$ mass concentration to PM_{10} was 11.86%. In comparison, the total mass concentration of PM_{10} at the outlet of desulfurization was 3.79 mg/m^3, the total mass concentration of $PM_{2.5}$ was 0.80 mg/m^3, and the ratio of $PM_{2.5}$ mass concentration to PM_{10} was 21.22%. The ratio of

$PM_{2.5}$ mass concentration to PM_{10} increased by 9.36% before and after WFGD. The capture efficiency of WFGD was 78.20% for PM_{10} and 61.00% for $PM_{2.5}$.

At the flue gas temperature of 100 °C, the total mass concentration of PM_{10} at the inlet of WFGD was 14.31 mg/m^3, whereas the total mass concentration of $PM_{2.5}$ was 4.18 mg/m^3, and the ratio of $PM_{2.5}$ mass concentration to PM_{10} was 29.21%. The total mass concentration of PM_{10} at the outlet of WFGD was 4.52 mg/m^3, the total mass concentration of $PM_{2.5}$ was 1.61 mg/m^3, and the ratio of $PM_{2.5}$ mass concentration to PM_{10} was 35.54%. The ratio of $PM_{2.5}$ mass concentration to PM_{10} increased by 6.33% before and after WFGD. The capture efficiency of WFGD was 68.39% for PM_{10} and 61.54% for $PM_{2.5}$.

Figure 8b shows that the mass concentration of $PM_{0.5\sim10}$ is reduced after desulfurization at both 140 °C and 100 °C flue gas temperatures. However, for $PM_{0.5}$, the concentration increases after desulfurization at 140 °C flue gas temperature and decreases after desulfurization at 100 °C flue gas temperature. The higher inlet flue gas temperature leads to an increase in the fine particle concentration at the WFGD outlet, which is consistent with the findings of his study [31]. This phenomenon is mainly attributed to the large temperature difference between the flue gas and the sprayed desulfurization slurry under high flue gas temperature conditions. When the flue gas comes into contact with the desulfurization slurry in the desulfurization tower, the evaporation of the desulfurization slurry increases the water content of the gas and reduces the gas temperature, which depends, to a large extent, on the temperature difference between the flue gas and the desulfurization slurry [40]. During the heat exchange between the flue gas and the desulfurization slurry, the thermal energy of the slurry particles formed by spraying increases, making them more easily carried out by the airflow. In addition, the roof-type mist eliminator is highly efficient for capturing $PM_{0.5\sim10}$, but has low efficiency for capturing $PM_{0.5}$.

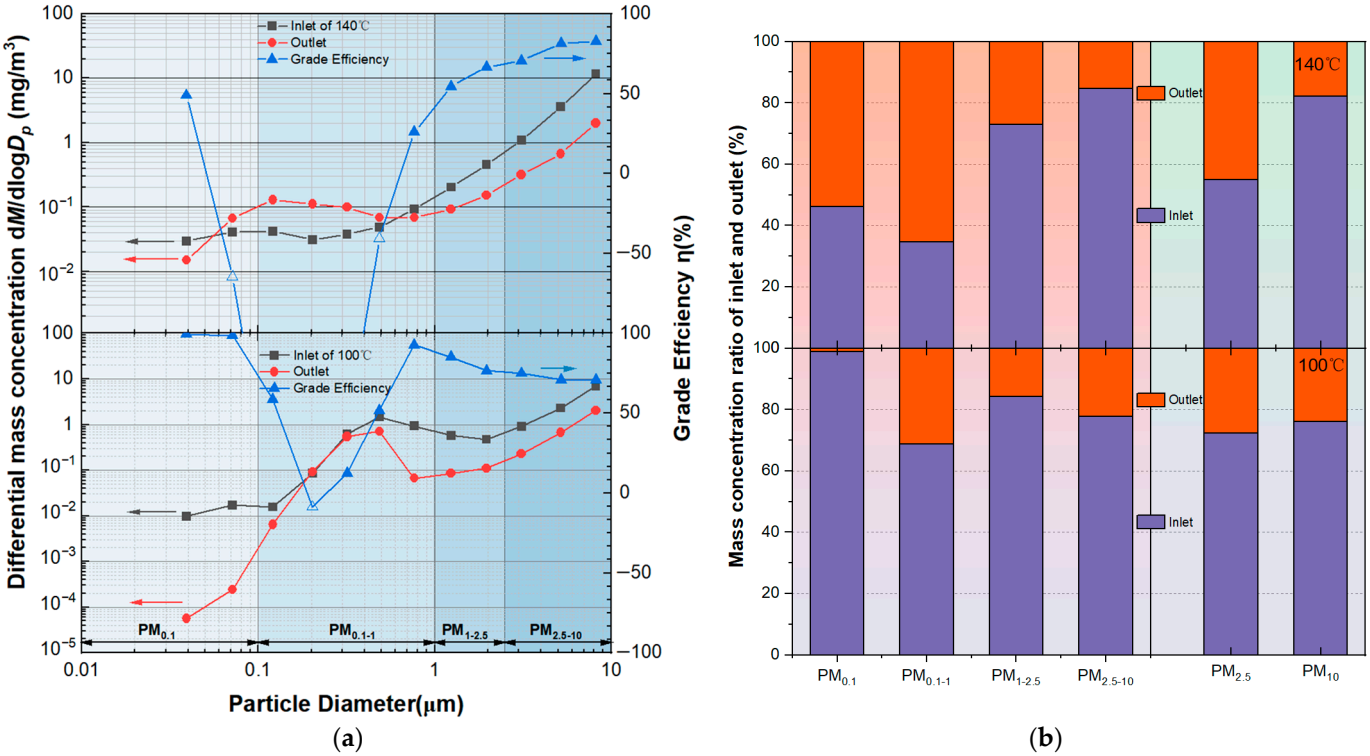

Figure 8. (**a**) Particle size distributions and grade efficiency of PM_{10}, (**b**) emission ratio of particles with different diameter at the inlet and outlet of different inlet flue gas temperature in Plant C.

3.4.3. The Influence of the Different PM Concentrations at the Desulfurization Inlet

In Power Plant C, Unit 4, the flue gas temperature at the inlet of the electric precipitator and wet desulfurization system is around 110 °C. By adjusting the electric field operation

parameters of the electric precipitator, two PM_{10} mass concentration levels are formed at the wet desulfurization inlet: high and low, as shown in Figure 9a.

Under high concentration conditions, the total PM_{10} mass concentration at the desulfurization inlet is 19.32 mg/m^3, with a total $PM_{2.5}$ mass concentration of 4.68 mg/m^3, and the proportion of $PM_{2.5}$ mass concentration to PM_{10} is 24.21%. Under low concentration conditions, the total PM_{10} mass concentration at the WFGD inlet is 8.40 mg/m^3, with a total $PM_{2.5}$ mass concentration of 1.77 mg/m^3, and the proportion of $PM_{2.5}$ mass concentration to PM_{10} is 21.09%.

Figure 9b shows the $PM_{2.5}$ and PM_{10} ratio at the WFGD inlet and outlet under high and low concentration conditions. After WFGD treatment, the PM_{10} mass concentration is reduced by 79.72% and $PM_{2.5}$ mass concentration is reduced by 63.80% under a high-concentration WFGD inlet PM_{10} mass concentration of about 20 mg/m^3. Under a low-concentration WFGD inlet PM_{10} mass concentration < 10 mg/m^3, the PM_{10} mass concentration is reduced by 32.03%, but the $PM_{2.5}$ mass concentration increases by 14.01%.

The efficiency of PM_{10} capture by WFGD is dependent on the mass concentration of PM_{10} at the WFGD inlet. The higher the mass concentration of PM_{10} at the inlet, the greater the capture efficiency. This is because a higher mass concentration results in a greater number concentration, leading to an increased likelihood of collision and combination between particulate matter and slurry particles. However, for $PM_{2.5}$, a low concentration at the WFGD inlet causes a significant decrease in number concentration, making it difficult to capture $PM_{2.5}$ through WFGD. In addition, the secondary carrying effect of airflow increases $PM_{2.5}$ emissions at the WFGD outlet.

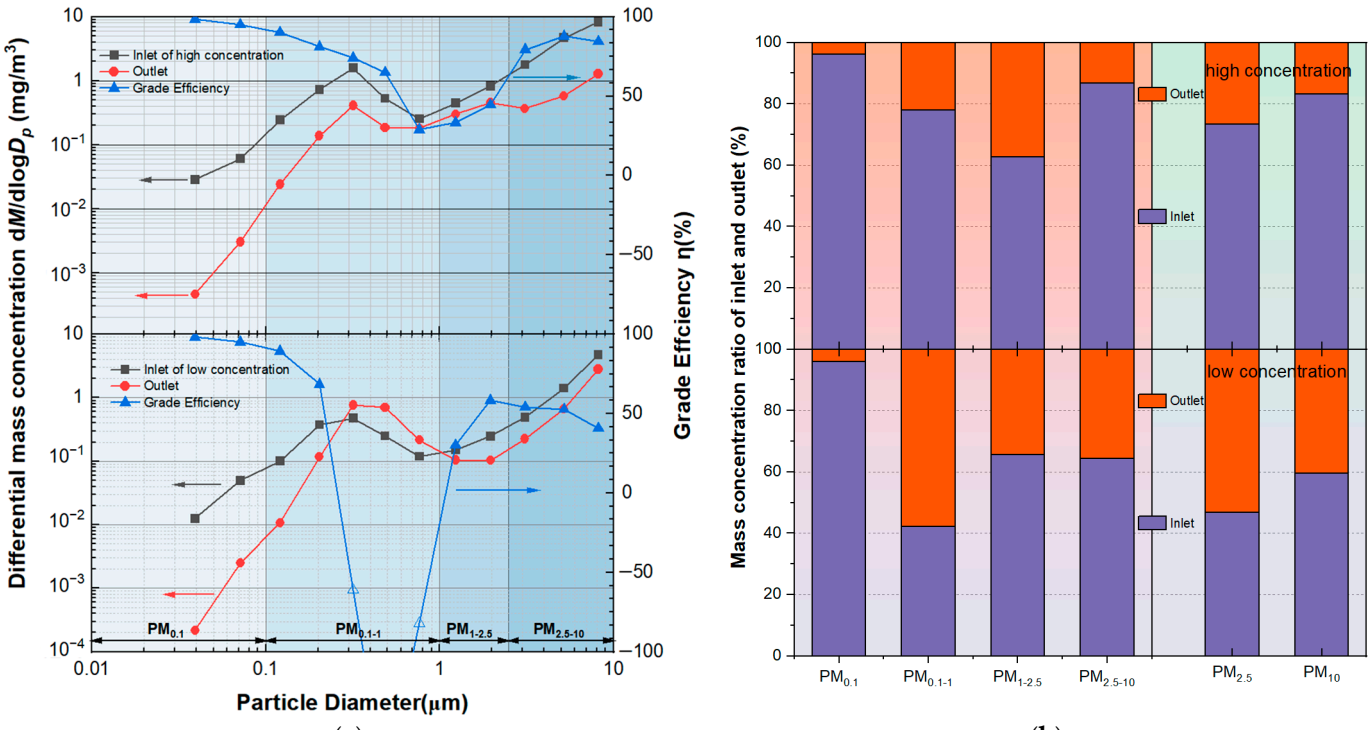

(**a**) (**b**)

Figure 9. (**a**) Particle size distributions and grade efficiency of PM_{10}, (**b**) emission ratio of particles with different diameter at the inlet and outlet of different inlet flue gas concentration in Plant C.

3.5. Summary

In this study, data from the experimental power plant were collected and analyzed. Figure 10a displays the statistical results of the ratio of $PM_{2.5}$ mass concentration to PM_{10} at the inlet and outlet of wet desulfurization. The average ratio of $PM_{2.5}$ mass concentration to PM_{10} at the WFGD inlet is 16.25%, ranging from 6.5% to 28.74%, whereas the average ratio at the WFGD outlet is 28.11%, ranging from 17.38% to 64%. The ratio of $PM_{2.5}$ mass

concentration to PM_{10} at the WFGD outlet is significantly higher than that at the inlet, indicating particle size selectivity of the WFGD for the capture of particulate matter.

Figure 10b shows the statistical results of the capture efficiency of PM_{10} and $PM_{2.5}$ by WFGD. The average capture efficiency of PM_{10} by wet desulfurization is 51.39%, whereas the capture efficiency of $PM_{2.5}$ is about 16.88%. WFGD has a significant effect on capturing large particle size (PM_{10}) compared to small particle size ($PM_{2.5}$).

Figure 10c displays the inlet and outlet concentrations of $PM_{2.5}$ and PM_{10} in the WFGD tower at different plant operating capacities and the percentage of $PM_{2.5}$ relative to PM_{10}. The results indicate that the higher the operating capacity, the higher the inlet PM_{10} concentration, the lower the $PM_{2.5}$ concentration, and the smaller the $PM_{2.5}$ to PM_{10} ratio. After wet desulfurization, the PM_{10} export concentration decreases significantly at different operating capacities, whereas the $PM_{2.5}$ export concentration does not change significantly. Furthermore, the proportion of $PM_{2.5}$ to PM_{10} is generally higher than that at the inlet.

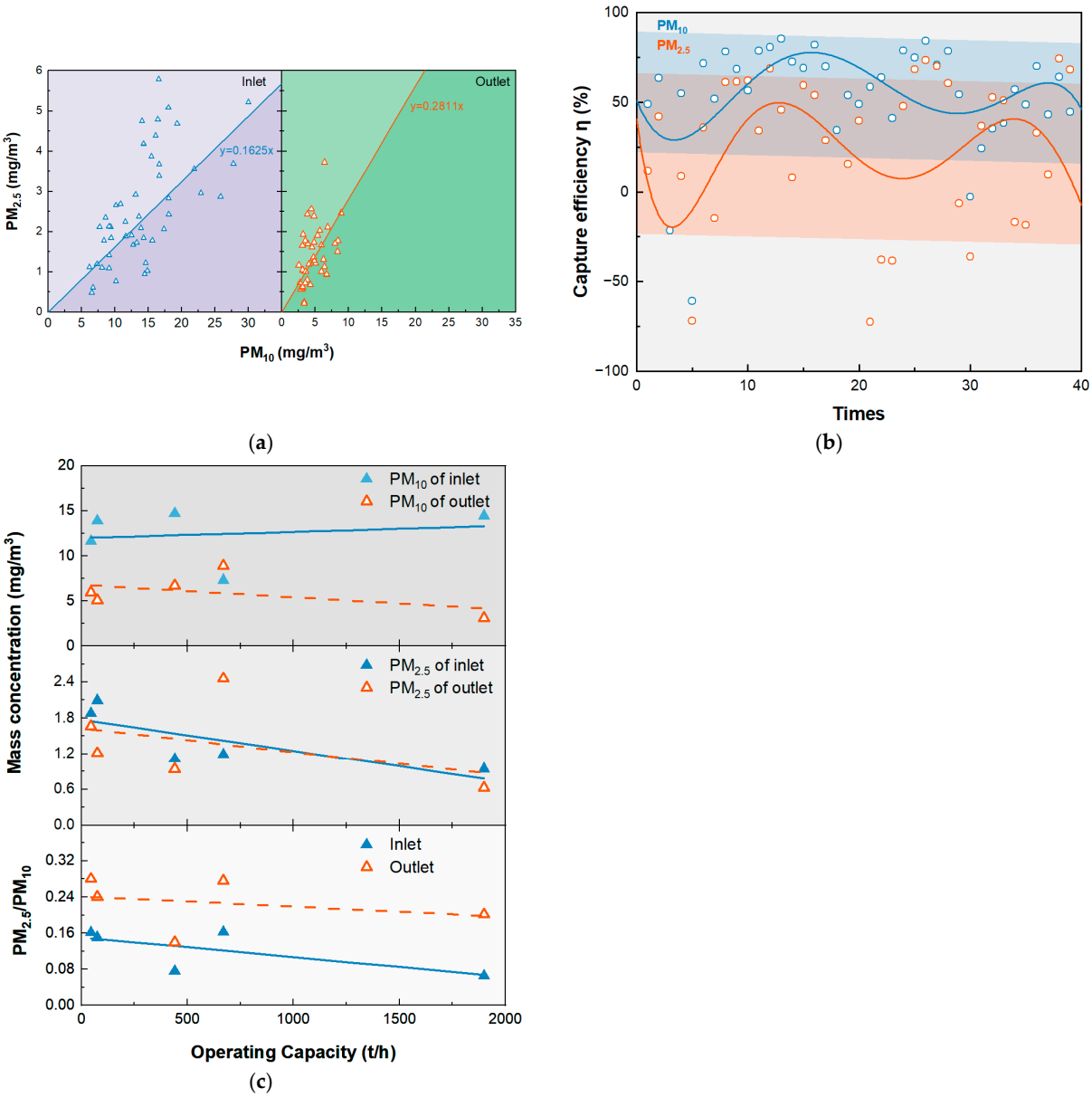

Figure 10. (**a**) PM_{10} and $PM_{2.5}$ mass concentration at inlet and outlet of WFGD, (**b**) capture efficiency of WFGD for PM_{10} and $PM_{2.5}$, and (**c**) mass concentration and ratio of $PM_{2.5}$ and PM_{10} at the inlet and outlet of the WFGD with different operating capacity.

4. Conclusions

In this study, we investigated the effects of WFGD on the particle size distribution and grade efficiency of PM_{10} in five different plants. Our main findings can be summarized as follows:

(1) The ELPI is an effective test method with more concentrated distribution, lower bias, and higher confidence in the test data of particle matter concentration than filter membrane sampler and filter cartridge sampler.
(2) WFGD showed significant capture efficiency for PM_{10} compared to $PM_{2.5}$, indicating that WFGD has particle size selectivity for the capture of particulate matter, with a better capture effect on larger particles and poorer capture effect on smaller particles.
(3) The three-stage roof-type mist eliminator in the tower of WFGD had higher PM_{10} capture efficiency than the conventional mechanical grid mist eliminator and two-stage ridge-type mist eliminator.
(4) Compared to the two-layer spray, the four-layer spray in the WFGD tower is more beneficial in reducing PM_{10} and $PM_{2.5}$ emissions, but its capture efficiency for submicron particles is lower because more small droplets are entrained.
(5) The PM_{10} capture efficiency of WFGD is affected by WFGD inlet flue gas temperature and particle matter concentration. Higher inlet flue gas temperature and lower inlet particle matter concentration can both increase WFGD outlet $PM_{0.1\sim1}$ emissions.

Author Contributions: A.W.: Conceptualization, Methodology, Software, Validation, Investigation, Data Curation, Writing—Original Draft Preparation, Writing—Review and Editing, Visualization. S.L.: Conceptualization, Methodology, Software, Validation, Formal Analysis, Resources, Data Curation, Writing—Original Draft Preparation, Writing—Review and Editing, Visualization, Supervision, Project Administration, Funding Acquisition. Q.Z.: Conceptualization, Methodology, Investigation, Data Curation, Formal Analysis. S.Z. (Shuo Zhang): Conceptualization, Software, Validation, Data Curation, Writing—Original Draft Preparation. S.Z. (Shihao Zhang): Conceptualization, Software, Validation, Investigation. Z.W.: Software, Validation, Investigation, Data Curation. Z.L.: Resources, Writing—Review and Editing, Supervision, Project Administration, Funding Acquisition. K.Y.: Resources, Writing—Review and Editing, Supervision, Project Administration, Funding Acquisition. All authors have read and agreed to the published version of the manuscript.

Funding: This research was supported by the Zhejiang Provincial Natural Science Foundation of China (Grant No. LQ22E020004) and Shanxi-Zheda Institute of Advanced Materials and Chemical Engineering (Grant No. 2021ST-AT-002).

Data Availability Statement: Data will be made available on request.

Acknowledgments: This work was supported by the Zhejiang Provincial Natural Science Foundation of China (Grant No. LQ22E020004). The authors also thank our colleagues and other students for their participation in this work.

Conflicts of Interest: The authors declare that they have no known competing financial interest or personal relationships that could have appeared to influence the work reported in this paper.

References

1. Zheng, K.; Liu, J.; Zhang, J.-F.; Hao, W. Assessment method for the prevention effectiveness of PM2.5 based on the optimization development of coal-fired power generation. In Proceedings of the IOP Conference Series: Earth and Environmental Science, Sanya, China, 21–23 November 2016; Volume 52, p. 012076.
2. Korzeniewska, A.; Szramowiat, K.; Gołaś, J. An overview of some challenges in the studies in the emission of particulate matter. In Proceedings of the IOP Conference Series: Earth and Environmental Science, Krakow, Poland, 14–17 November 2017; Volume 214, p. 012119.
3. Burnett, R.T.; Pope, C.A.; Ezzati, M.; Olives, C.; Lim, S.S.; Mehta, S.; Shin, H.H.; Singh, G.; Hubbell, B.; Brauer, M.; et al. An integrated risk function for estimating the global burden of disease attributable to ambient fine particulate matter exposure. *Environ. Health Perspect.* **2014**, *122*, 397–403. [CrossRef]
4. Zhang, Q.; He, K.; Huo, H. Cleaning China's air. *Nature* **2012**, *484*, 161–162. [CrossRef] [PubMed]
5. Cheng, Y.; Zheng, G.; Wei, C.; Mu, Q.; Zheng, B.; Wang, Z.; Gao, M.; Zhang, Q.; He, K.; Carmichael, G.; et al. Reactive nitrogen chemistry in aerosol water as a source of sulfate during haze events in China. *Sci. Adv.* **2016**, *2*, e1601530. [CrossRef] [PubMed]

6. Zhang, S.; Liu, Z.; Li, S.; Tu, X.; Zhang, S.; Xu, W.; Shen, X.; Huang, D.; Gao, L.; Yan, K. Soil remediation via DBD induced multiple pollutants cleaning. *Int. J. Plasma Environ. Sci. Technol* **2004**, *16*, 7pp.
7. Wang, K.; Wang, S.; Liu, L.; Yue, H.; Zhang, R.; Tang, X. Environmental co-benefits of energy efficiency improvement in coal-fired power sector: A case study of Henan Province, China. *Appl. Energy* **2016**, *184*, 810–819. [CrossRef]
8. Niu, Y.; Yan, B.; Liu, S.; Liang, Y.; Dong, N.; Hui, S. Ultra-fine particulate matters (PMs)formation during air and oxy-coal combustion: Kinetics study. *Appl. Energy* **2018**, *218*, 46–53. [CrossRef]
9. Li, M.; Patiño-Echeverri, D.; Zhang, J.J. Policies to promote energy efficiency and air emissions reductions in China's electric power generation sector during the 11th and 12th five-year plan periods: Achievements, remaining challenges, and opportunities. *Energy Policy* **2019**, *125*, 429–444. [CrossRef]
10. State Development and Reform Commission, Coal Energy Saving, Emission Reduction Upgrade and Reform Action Plan (2014–2020). Available online: https://www.gov.cn/gongbao/content/2015/content_2818468.htm (accessed on 25 April 2023).
11. Ruan, R.; Liu, H.; Tan, H.; Yang, F.; Li, Y.; Duan, Y.; Zhang, S.; Lu, X. Effects of APCDs on PM emission: A case study of a 660 MW coal-fired unit with ultralow pollutants emission. *Appl. Therm. Eng.* **2019**, *155*, 418–427. [CrossRef]
12. Flagiello, D.; Erto, A.; Lancia, A.; Di Natale, F. Dataset of wet desulphurization scrubbing in a column packed with Mellapak 250 X. *Data Brief* **2020**, *33*, 106383. [CrossRef]
13. Muzio, L.J.; Quartucy, G.C.; Cichanowiczy, J.E. Overview and status of post-combustion NOx control: SNCR, SCR and hybrid technologies. *Int. J. Environ. Pollut.* **2002**, *17*, 4–30. [CrossRef]
14. Wang, Y.; Gao, W.; Zhang, H.; Shao, L.; Wu, Z.; Li, L.; Sun, D.; Zheng, C.; Gao, X. Enhanced particle precipitation from flue gas containing ultrafine particles through precharging. *Process Saf. Environ. Prot.* **2020**, *144*, 111–122. [CrossRef]
15. Yi, H.; Guo, X.; Hao, J.; Duan, L.; Li, X. Characteristics of inhalable particulate matter concentration and size distribution from power plants in China. *J. Air Waste Manag. Assoc.* **2006**, *56*, 1243–1251. [CrossRef]
16. Zhang, S.; Shen, X.; Tian, Y.; Fu, Y.; Li, M.; Li, S.; Zhu, W.; Ke, Y.; Yan, K. The turbulent-flow-assisted electrostatic collection and alignment of recycled short-chopped carbon fiber in gaseous phase. *Sep. Purif. Technol.* **2023**, *305*, 122518. [CrossRef]
17. Tian, Y.; Li, M.; Fu, Y.; Liu, L.; Li, S.; Zhu, W.; Ke, Y.; Yan, K. Development and experimental investigation of the narrow-gap coated electrostatic precipitator with a shield pre-charger for indoor air cleaning. *Sep. Purif. Technol.* **2023**, *309*, 123114. [CrossRef]
18. Zhu, J.; Xu, Y.; Jiang, A.; Mo, H. Test and Study on Performance of Wet FGD Coordinated Particulate Matter Control for Ultra-Low Pollutants Emission. *Electr. Power* **2017**, *50*, 168–172. (In Chinese)
19. Huang, Y.; Shen, H.; Chen, H.; Wang, R.; Zhang, Y.; Su, S.; Chen, Y.; Lin, N.; Zhuo, S.; Zhong, Q.; et al. Quantification of global primary emissions of PM2.5, PM10, and TSP from combustion and industrial process sources. *Environ. Sci. Technol.* **2014**, *48*, 13834–13843. [CrossRef]
20. Guttikunda, S.K.; Jawahar, P. Atmospheric emissions and pollution from the coal-fired thermal power plants in India. *Atmos. Environ.* **2014**, *92*, 449–460. [CrossRef]
21. Mokhtar, M.M.; Hassim, M.H.; Taib, R.M. Health risk assessment of emissions from a coal-fired power plant using AERMOD modelling. *Process Saf. Environ. Prot.* **2014**, *92*, 476–485. [CrossRef]
22. Di Natale, F.; Carotenuto, C.; Parisi, A.; Flagiello, D.; Lancia, A. Wet electrostatic scrubbing for flue gas treatment. *Fuel* **2022**, *325*, 124888. [CrossRef]
23. Li, X.; Han, J.; Liu, Y.; Dou, Z.; Zhang, T.-A. Summary of research progress on industrial flue gas desulfurization technology. *Sep. Purif. Technol.* **2022**, *281*, 119849. [CrossRef]
24. Zhu, J.; Ye, S.-C.; Bai, J.; Wu, Z.-Y.; Liu, Z.-H.; Yang, Y.-F. A concise algorithm for calculating absorption height in spray tower for wet limestone–gypsum flue gas desulfurization. *Fuel Process. Technol.* **2015**, *129*, 15–23. [CrossRef]
25. Sun, Y.; Xie, J.; Huang, W.; Li, G.; Li, S.; Cui, P.; Xu, H.; Qu, Z.; Yan, N. Novel product-adjustable technology using Wellman-Lord method coupled with sodium-alkali for SO2 removal and regeneration from smelting gas. *Fuel* **2021**, *288*, 119714. [CrossRef]
26. del Valle-Zermeño, R.; Niubó, M.; Formosa, J.; Guembe, M.; Aparicio, J.; Chimenos, J. Synergistic effect of the parameters affecting wet flue gas desulfurization using magnesium oxides by-products. *Chem. Eng. J.* **2015**, *262*, 268–277. [CrossRef]
27. Carotenuto, C.; Di Natale, F.; Lancia, A. Wet electrostatic scrubbers for the abatement of submicronic particulate. *Chem. Eng. J.* **2010**, *165*, 35–45. [CrossRef]
28. Liu, X.; Xu, Y.; Zeng, X.; Zhang, Y.; Xu, M.; Pan, S.; Zhang, K.; Li, L.; Gao, X. Field measurements on the emission and removal of PM2.5 from coal-fired power stations: 1. Case study for a 1000 MW ultrasupercritical utility boiler. *Energy Fuels* **2016**, *30*, 6547–6554. [CrossRef]
29. Li, J.; Qi, Z.; Li, M.; Wu, D.; Zhou, C.; Lu, S.; Yan, J.; Li, X. Physical and chemical characteristics of condensable particulate matter from an ultralow-emission coal-fired power plant. *Energy Fuels* **2017**, *31*, 1778–1785. [CrossRef]
30. Sui, Z.; Zhang, Y.; Peng, Y.; Norris, P.; Cao, Y.; Pan, W.P. Fine particulate matter emission and size distribution characteristics in an ultra-low emission power plant. *Fuel* **2016**, *185*, 863–871. [CrossRef]
31. Wu, H.; Yang, L.J.; Yan, J.P.; Hong, G.X.; Yang, B. Improving the removal of fine particles by heterogeneous condensation during WFGD processes. *Fuel Process. Technol.* **2016**, *145*, 116–122. [CrossRef]
32. Sui, Z.; Zhang, Y.; Peng, Y.; Norris, P.; Cao, Y.; Pan, W.-P. Effects of wet flue gas desulfurization and wet electrostatic precipitator on particulate matter and sulfur oxide emission in coal-fired power plants. *Energy Fuels* **2020**, *34*, 16423–16432.

33. State Environmental Protection Administration of China, The Determination of Particulates and Sampling Methods of Gaseous Pollutants Emitted from Exhaust Gas of Stationary Source. Available online: https://www.mee.gov.cn/ywgz/fgbz/bz/bzwb/jcffbz/199603/t19960306_67508.shtml (accessed on 25 April 2023).
34. Marjamäki, M.; Lemmetty, M.; Keskinen, J. ELPI Response and data reduction I: Response functions. *Aerosol Sci. Technol.* **2005**, *39*, 575–582. [CrossRef]
35. Yli-Ojanperä, J.; Kannosto, J.; Marjamäki, M.; Keskinen, J. Improving the nanoparticle resolution of the ELPI. *Aerosol Air Qual. Res.* **2010**, *10*, 360–366. [CrossRef]
36. Linak, W.P.; Miller, C.A.; Wendt, J.O.L. Comparison of Particle Size Distributions and Elemental Partitioning from the Combustion of Pulverized Coal and Residual Fuel Oil. *J. Air Waste Manag. Assoc.* **2000**, *50*, 1532–1544. [CrossRef]
37. Wu, Y.; Xu, Z.; Liu, S.; Tang, M.; Lu, S. Emission Characteristics of Particulate Matter from Coal-Fired Power Units with Different Load Conditions. *Water Air Soil Pollut* **2022**, *233*, 447. [CrossRef]
38. Xu, Z.; Wu, Y.; Huang, X.; Liu, S.; Tang, M.; Lu, S. Study on the control of condensable particulate matter by spraying activated carbon combined with electrostatic precipitator. *Atmos. Pollut. Res.* **2022**, *13*, 101544. [CrossRef]
39. Li, Z.; Jiang, J.; Ma, Z.; Fajardo, O.A.; Deng, J.; Duan, L. Influence of flue gas desulfurization (FGD) installations on emission characteristics of PM2.5 from coal-fired power plants equipped with selective catalytic reduction (SCR). *Environ. Pollut.* **2017**, *230*, 655–662. [CrossRef]
40. Jingjing, B.; Linjun, Y.; Jinpei, Y.; Guilong, X.; Bin, L.; Chengyun, X. Experimental study of fine particles removal in the desulfurated scrubbed flue gas. *Fuel* **2013**, *108*, 73–79. [CrossRef]